



Contents lists available at ScienceDirect

Inorganica Chimica Acta

journal homepage: [www.elsevier.com/locate/ica](http://www.elsevier.com/locate/ica)

## Ruthenium(II)-arene complexes with dibenzoylmethane induce apoptotic cell death in multiple myeloma cell lines

Riccardo Pettinari<sup>a,\*</sup>, Fabio Marchetti<sup>b</sup>, Agnese Petrini<sup>a</sup>, Claudio Pettinari<sup>a</sup>, Giulio Lupidi<sup>a</sup>, Belén Fernández<sup>c</sup>, Antonio Rodríguez Diéguez<sup>c</sup>, Giorgio Santoni<sup>a</sup>, Massimo Nabissi<sup>a</sup>

<sup>a</sup>School of Pharmacy, University of Camerino, via S. Agostino 1, 62032 Camerino, MC, Italy

<sup>b</sup>School of Science and Technology, University of Camerino, via S. Agostino 1, 62032 Camerino, MC, Italy

<sup>c</sup>Departamento de Química Inorgánica, Universidad de Granada, Avda Fuentenueva s/n, 18071 Granada, Spain

### ARTICLE INFO

#### Article history:

Received 26 January 2016

Received in revised form 11 April 2016

Accepted 18 April 2016

Available online xxxx

#### Keywords:

Ru(II)-arene

Dibenzoylmethane

RAPTA

DNA interaction studies

Protein binding studies

Multiple myeloma

### ABSTRACT

A series of ruthenium(II) arene complexes (arene = *p*-cymene, hexamethylbenzene and benzene) containing dibenzoylmethane ligand (DBMH) of formula [(arene)Ru(DBM)Cl] and their ionic derivatives bearing PTA (1,3,5-triaza-7-phosphaadamantane), of formula [(arene)Ru(DBM)(PTA)]X (X = PF<sub>6</sub><sup>-</sup> or SO<sub>3</sub>CF<sub>3</sub><sup>-</sup>) have been synthesized and fully characterized. The solid-state structures of five complexes have been determined by single-crystal X-ray diffraction. These ruthenium materials exhibit intense photoluminescence emission at room temperature in the solid state. All complexes effectively bind to calf thymus DNA through intercalative/electrostatic interactions with more affinity for DNA minor groove. Finally, the anti-tumor activity of both ligand and complexes was evaluated against the U266 and RPMI human multiple myeloma cell lines, and some of them showed a cytotoxic and pro-apoptotic effect toward both cell lines.

© 2016 Elsevier B.V. All rights reserved.

### 1. Introduction

Half-sandwich η<sup>6</sup>-arene ruthenium complexes are currently attracting increasing attention for their potential applications as metallopharmaceuticals in cancer therapy [1–4]. The hydrophobic arene ligand can facilitate the diffusion of the complexes through the lipophilic cell membrane and the three remaining Ru coordination sites can be filled with several kinds of ligands [5,6]. Recent developments on this field by several authors deal mainly on the use of chelating N,N'-donor ligands, such as complexes from Sadler's group [7–10], or complexes with the P-donor ligand PTA investigated by Dyson's group [11–14]. However, also reports on arene Ru(II) complexes with O,O'-donor ligands are attracting increasing attention, as many different possibilities are available to tune both the chelating ring from four to six-membered and the steric crowding of such ligands [15–20]. Some papers have focused on β-diketonate complexes, firstly investigated by Sadler who reported that replacement of neutral ethylenediamine (en) by anionic acetylacetonate (acac) as the chelating ligand not only increases the rate and extent of hydrolysis but also changes the nucleobase specificity [21,22]. Some of these arene-Ru(II)

β-diketonates, containing also the complex [(*p*-cym)Ru(DBM)Cl] (1) reported in this work, possess good activity toward A2780 human ovarian cells [23]. The combination of dibenzoylmethane and PTA ligands was also investigated by Dyson, who reported a series of cationic arene-Ru(II) complexes, quite soluble in water with a high cytotoxicity towards A2780 human ovarian cancer cells and also against A549 lung carcinoma [24].

Multiple myeloma (MM) remains almost an incurable disease, and several new drugs are currently undergoing evaluation for disease control [25]. As a part of our continuing research in ruthenium chemistry, here we report the synthesis of a series of arene-Ru(II) complexes (arene = *p*-cymene, hexamethylbenzene, and benzene) with dibenzoylmethane (DMBH) and their ionic derivatives with the PTA ligand and two external counterions, namely PF<sub>6</sub><sup>-</sup> and SO<sub>3</sub>CF<sub>3</sub><sup>-</sup> anions. The choice to use different counterions with the same cationic complex was planned with the goal to investigate their potential influence on cytotoxicity. Their radical scavenging ability (DPPH), DNA and BSA-protein interactions and also the cytotoxicity toward U266 and RPMI multiple myeloma (MM) cell lines have been evaluated for the first time, differently from previous studies [23,24].

Our interest on these tumor lines deals on the fact that they have been previously characterized for their cytogenetic abnormalities (loss of 17p), which is associated with a poor outcome. In fact,

\* Corresponding author. Tel.: +39 0737402338.

E-mail address: [riccardo.pettinari@unicam.it](mailto:riccardo.pettinari@unicam.it) (R. Pettinari).

del(17p) is the most important molecular finding for prognostication as it linked to an aggressive disease phenotype [26].

## 2. Experimental

### 2.1. Materials and methods

The dimers [(arene)RuCl<sub>2</sub>]<sub>2</sub> (arene = *p*-cym, hmb, benzene) and dibenzoylmethane were purchased from Aldrich and were used as received. All other materials were obtained from commercial sources and were used as received. IR spectra were recorded from 4000 to 30 cm<sup>-1</sup> on a PerkinElmer Frontier FT-IR instrument. <sup>1</sup>H, <sup>13</sup>C and <sup>31</sup>P NMR spectra were recorded on a 400 Mercury Plus Varian instrument operating at room temperature (400 MHz for <sup>1</sup>H and 100 MHz for <sup>13</sup>C relative to TMS, and 162 MHz relative to 85% H<sub>3</sub>PO<sub>4</sub>). Positive and negative ion electrospray ionization mass spectra (ESI-MS) were obtained on a Series 1100 MSI detector HP spectrometer using methanol as the mobile phase. Solutions (3 mg/mL) analysis were prepared using reagent-grade methanol. Masses and intensities were compared to those calculated using IsoPro Isotopic Abundance Simulator, version 2.1.28. Melting points are uncorrected and were recorded on a STMP3 Stuart scientific instrument and on a capillary apparatus. Samples for microanalysis were dried in vacuo to constant weight (20 °C, ca. 0.1 Torr) and analyzed on a Fisons Instruments 1108 CHNS-O elemental analyzer. Electrical conductivity measurements (Λ<sub>m</sub>, reported as S cm<sup>2</sup> mol<sup>-1</sup>) of acetonitrile solutions of the complexes were recorded using a Eutech Instruments CON2700 at room temperature. UV-Vis spectra of the proligands and complexes were performed with a Varian Cary1 spectrometer at 20 °C. The fluorescence of the proligands and complexes was analyzed using a Hitachi F-4500 spectrofluorimeter at 20 °C.

### 2.2. Synthesis of ruthenium complexes

#### 2.2.1. [(*p*-cym)Ru(DBM)Cl] (1)

The compound was synthesized using a modified literature method [23]. Dibenzoylmethane (DBMH, 224.0 mg, 1.00 mmol) was dissolved in methanol (20 mL) and KOH (56.1 mg, 1.00 mmol) was added. The mixture was stirred for 1 h at room temperature and then [(*p*-cym)RuCl<sub>2</sub>]<sub>2</sub> (244.9 mg, 0.40 mmol) was added. The resulting mixture was stirred for 24 h at room temperature. The solvent was removed under reduced pressure, dichloromethane (10 mL) was added and the mixture was filtered to remove potassium chloride. The solution was concentrated to 2 mL and then an excess of *n*-hexane resulted in precipitation of a red powder (332.0 mg, 0.67 mmol, yield 84%) which was identified as **1**. It is soluble in alcohols, acetone, acetonitrile, chlorinated solvents, DMF and DMSO and slightly soluble in diethyl ether. Mp: 197–198 °C. *Anal. Calc.* for C<sub>25</sub>H<sub>25</sub>ClO<sub>2</sub>Ru: C, 60.79; H, 5.10. *Found:* C, 60.74; H, 5.08. Λ<sub>m</sub> (CD<sub>3</sub>CN, 298 K, 10<sup>-4</sup> mol/L): 36 S cm<sup>2</sup> mol<sup>-1</sup>. IR (cm<sup>-1</sup>): 3063–2871w ν(C–H), 1591m, 1520vs ν(C=O; C=C), 1371s, 1306s, 724s, 280m ν(Ru–Cl). <sup>1</sup>H NMR (CDCl<sub>3</sub>, 293 K): δ 1.41 (d, 6H, CH<sub>3</sub>C<sub>6</sub>H<sub>4</sub>CH(CH<sub>3</sub>)<sub>2</sub>, <sup>3</sup>J = 7.2 Hz), 2.34 (s, 3H, CH<sub>3</sub>C<sub>6</sub>H<sub>4</sub>CH(CH<sub>3</sub>)<sub>2</sub>), 3.02 (sept, 1H, CH<sub>3</sub>C<sub>6</sub>H<sub>4</sub>CH(CH<sub>3</sub>)<sub>2</sub>, <sup>3</sup>J = 7.2 Hz), 5.31 (d, 2H, CH<sub>3</sub>C<sub>6</sub>H<sub>4</sub>CH(CH<sub>3</sub>)<sub>2</sub>, <sup>3</sup>J = 6.0 Hz), 5.59 (d, 2H, CH<sub>3</sub>C<sub>6</sub>H<sub>4</sub>CH(CH<sub>3</sub>)<sub>2</sub>, <sup>3</sup>J = 6.0 Hz), 6.44 (s, 1H, CH of DBM), 7.39 (m, 6H, Ph of DBM), 7.91 (d, 4H, Ph of DBM, <sup>3</sup>J = 7.2 Hz). <sup>13</sup>C NMR (CDCl<sub>3</sub>, 293 K): δ 18.3 (s, CH<sub>3</sub>C<sub>6</sub>H<sub>4</sub>CH(CH<sub>3</sub>)<sub>2</sub>), 22.7 (s, CH<sub>3</sub>C<sub>6</sub>H<sub>4</sub>CH(CH<sub>3</sub>)<sub>2</sub>), 31.1 (s, CH<sub>3</sub>C<sub>6</sub>H<sub>4</sub>CH(CH<sub>3</sub>)<sub>2</sub>), 79.6, 83.4 (s, CH<sub>3</sub>C<sub>6</sub>H<sub>4</sub>CH(CH<sub>3</sub>)<sub>2</sub>), 93.6 (s, CH of DBM), 97.7, 100.0 (s, CH<sub>3</sub>C<sub>6</sub>H<sub>4</sub>CH(CH<sub>3</sub>)<sub>2</sub>), 127.5, 128.4, 131.2, 139.2 (s, Ph of DBM), 181.7 (s, C=O, DBM). ESI-MS (+) CH<sub>3</sub>OH (*m/z* (relative intensity, %)): 459 (100) [(*p*-cym)Ru(DBM)]<sup>+</sup>.

#### 2.2.2. [(hmb)Ru(DBM)Cl] (2)

The synthesis was performed as for **1** using a modified literature method [27] (yield 86%). Compound **2** is soluble in alcohols, acetone, acetonitrile, chlorinated solvents, DMF and DMSO and slightly soluble in diethyl ether. Mp: 279–281 °C. *Anal. Calc.* for C<sub>27</sub>H<sub>29</sub>ClO<sub>2</sub>Ru: C, 62.12; H, 5.60. *Found:* C, 62.15; H, 5.66. Λ<sub>m</sub> (CD<sub>3</sub>CN, 298 K, 10<sup>-4</sup> mol/L): 47 S cm<sup>2</sup> mol<sup>-1</sup>. IR (cm<sup>-1</sup>): 3013w ν(C–H), 1592m, 1543s, 1532vs ν(C=O; C=C), 1485m, 1454m, 1397s, 1373m, 1305m, 757s, 286m ν(Ru–Cl). <sup>1</sup>H NMR (CDCl<sub>3</sub>, 293 K): δ 2.15 (s, 18H, CH<sub>3</sub>(hmb)), 6.45 (s, 1H, CH of DBM), 7.40 (m, 6H, Ph of DBM), 7.96 (d, 4H, Ph of DBM, <sup>3</sup>J = 7.2 Hz). <sup>13</sup>C NMR (CDCl<sub>3</sub>, 293 K): δ 15.5 (s, CH<sub>3</sub>(hmb)), 90.7 (s, C<sub>6</sub>(hmb)), 93.0 (s, CH of DBM), 127.3, 128.3, 131.0, 139.5 (s, Ph of DBM), 180.9 (s, C=O, DBM). ESI-MS (+) CH<sub>3</sub>OH (*m/z* (relative intensity, %)): 487 (100) [(hmb)Ru(DBM)]<sup>+</sup>.

#### 2.2.3. [(benz)Ru(DBM)Cl] (3)

The synthesis was performed as for **1** using [(benz)RuCl<sub>2</sub>]<sub>2</sub> and keeping the reaction stirring at reflux for 24 h (yield 85%). Compound **3** is soluble in alcohols, acetone, acetonitrile, chlorinated solvents, DMF and DMSO and slightly soluble in diethyl ether. Mp: 223–225 °C. *Anal. Calc.* for C<sub>21</sub>H<sub>17</sub>ClO<sub>2</sub>Ru: C, 57.60; H, 3.91. *Found:* C, 57.49; H, 3.88. Λ<sub>m</sub> (CD<sub>3</sub>CN, 298 K, 10<sup>-4</sup> mol/L): 19 S cm<sup>2</sup> mol<sup>-1</sup>. IR (cm<sup>-1</sup>): 3062w ν(C–H), 1591m, 1545s, 1522vs ν(C=O; C=C), 1485m, 1451m, 1380s, 1373m, 1306w, 722s, 270s ν(Ru–Cl). <sup>1</sup>H NMR (CDCl<sub>3</sub>, 293 K): δ 5.74 (s, 6H, C<sub>6</sub>H<sub>6</sub>(benz)), 6.44 (s, 1H, CH of DBM), 7.41 (m, 6H, Ph of DBM), 7.90 (d, 4H, Ph of DBM, <sup>3</sup>J = 7.2 Hz). <sup>13</sup>C NMR (CDCl<sub>3</sub>, 293 K): 82.8 (s, C<sub>6</sub>H<sub>6</sub>(benz)), 94.0 (s, CH of DBM), 127.6, 128.3, 131.2, 139.1 (s, Ph of DBM), 182.1 (s, C=O, DBM). ESI-MS (+) CH<sub>3</sub>OH (*m/z* (relative intensity, %)): 403 (100) [(benz)Ru(DBM)]<sup>+</sup>.

#### 2.2.4. [(*p*-cym)Ru(DBM)(PTA)][SO<sub>3</sub>CF<sub>3</sub>] (4)

Compound **1** (271.7 mg, 0.55 mmol) was dissolved in methanol (20 mL) and AgSO<sub>3</sub>CF<sub>3</sub> (141.3 mg, 0.55 mmol) was added. The mixture was stirred for 1 h at room temperature and filtered to remove AgCl. PTA (PTA = 1,3,5-triaza-7-phosphaadamantane; 86.4 mg, 0.55 mmol) was then added to the filtrate which was stirred for 24 h at room temperature. Then the solution was dried by rotary evaporation and the crude product was obtained by precipitation using a mixture of dichloromethane and *n*-hexane. The yellow-brown powder obtained (319.6 mg, 0.42 mmol, yield 76%) was identified as **4**. It is soluble in alcohols, acetone, acetonitrile, chlorinated solvents, DMF and DMSO and rather soluble in water. Mp: 107–109 °C. *Anal. Calc.* for C<sub>32</sub>H<sub>37</sub>F<sub>3</sub>N<sub>3</sub>O<sub>5</sub>PRuS: C, 50.26; H, 4.88; N, 5.49. *Found:* C, 50.29; H, 4.92; N, 5.53. Λ<sub>m</sub> (CD<sub>3</sub>CN, 298 K, 10<sup>-4</sup> mol/L): 126 S cm<sup>2</sup> mol<sup>-1</sup>. IR (cm<sup>-1</sup>): 3064–2938w ν(C–H), 1590m, 1519vs ν(C=O; C=C), 1477m, 1374s, 1258vs, 1152s, 1030vs ν(SO<sub>3</sub>CF<sub>3</sub>), 971s, 946vs, 723s, 636s. <sup>1</sup>H NMR (CD<sub>3</sub>CN, 293 K): δ 1.31 (d, 6H, CH<sub>3</sub>C<sub>6</sub>H<sub>4</sub>CH(CH<sub>3</sub>)<sub>2</sub>, <sup>3</sup>J = 6.8 Hz), 2.08 (s, 3H, CH<sub>3</sub>C<sub>6</sub>H<sub>4</sub>CH(CH<sub>3</sub>)<sub>2</sub>), 2.71 (sept, 1H, CH<sub>3</sub>C<sub>6</sub>H<sub>4</sub>CH(CH<sub>3</sub>)<sub>2</sub>, <sup>3</sup>J = 6.8 Hz), 4.16 (s, 6H, NCH<sub>2</sub>P, PTA), 4.46 (s, 6H, NCH<sub>2</sub>N, PTA), 5.89 (d, 2H, CH<sub>3</sub>C<sub>6</sub>H<sub>4</sub>CH(CH<sub>3</sub>)<sub>2</sub>, <sup>3</sup>J = 6.4 Hz), 5.94 (d, 2H, CH<sub>3</sub>C<sub>6</sub>H<sub>4</sub>CH(CH<sub>3</sub>)<sub>2</sub>, <sup>3</sup>J = 6.4 Hz), 6.88 (s, 1H, CH of DBM), 7.53 (m, 4H, Ph of DBM), 7.63 (m, 2H, Ph of DBM), 8.00 (d, 4H, Ph of DBM, <sup>3</sup>J = 8.0 Hz). <sup>13</sup>C NMR (CD<sub>3</sub>CN, 293 K): δ 17.4 (s, CH<sub>3</sub>C<sub>6</sub>H<sub>4</sub>CH(CH<sub>3</sub>)<sub>2</sub>), 22.4 (s, CH<sub>3</sub>C<sub>6</sub>H<sub>4</sub>CH(CH<sub>3</sub>)<sub>2</sub>), 31.3 (s, CH<sub>3</sub>C<sub>6</sub>H<sub>4</sub>CH(CH<sub>3</sub>)<sub>2</sub>), 52.0 (d, PCH<sub>2</sub>N, PTA, J<sub>CP</sub> = 13.0 Hz), 73.1 (d, NCH<sub>2</sub>N, PTA, J<sub>CP</sub> = 7.7 Hz), 89.3, 90.7 (s, CH<sub>3</sub>C<sub>6</sub>H<sub>4</sub>CH(CH<sub>3</sub>)<sub>2</sub>), 96.5 (s, CH of DBM), 98.5, 105.5 (s, CH<sub>3</sub>C<sub>6</sub>H<sub>4</sub>CH(CH<sub>3</sub>)<sub>2</sub>), 128.4, 129.7, 133.1, 138.4 (s, Ph of DBM), 184.4 (s, C=O, DBM). <sup>31</sup>P NMR (CD<sub>3</sub>CN, 293 K): δ -27.9 (s, PTA). ESI-MS (+) CH<sub>3</sub>OH (*m/z* (relative intensity, %)): 616 (100) [(*p*-cym)Ru(DBM)(PTA)]<sup>+</sup>, 459 (20) [(*p*-cym)Ru(DBM)]<sup>+</sup>.

### 2.2.5. [(*p*-cym)(RuDBM)(PTA)][PF<sub>6</sub>] (5)

The synthesis was performed as for **4** using AgPF<sub>6</sub> (yield 73%). **5** is soluble in alcohols, acetone, acetonitrile, chlorinated solvents, DMF and DMSO and slightly soluble in water. Mp: 138–140 °C. *Anal. Calc.* for C<sub>31</sub>H<sub>37</sub>F<sub>6</sub>N<sub>3</sub>O<sub>2</sub>P<sub>2</sub>Ru: C, 48.95; H, 4.90; N, 5.52. Found: C, 48.91; H, 4.88; N, 5.49.  $\Lambda_M$  (CD<sub>3</sub>CN, 298 K, 10<sup>-4</sup> mol/L): 129 S cm<sup>2</sup> mol<sup>-1</sup>. IR (cm<sup>-1</sup>): 3059–2925w  $\nu$ (C–H), 1590m, 1519vs  $\nu$ (C=O; C=C), 1476m, 1373s, 1260m, 972s, 947s, 833vs  $\nu$ (PF<sub>6</sub>), 722s, 556s. <sup>1</sup>H NMR (CD<sub>3</sub>CN, 293 K):  $\delta$  1.31 (d, 6H, CH<sub>3</sub>C<sub>6</sub>H<sub>4</sub>CH(CH<sub>3</sub>)<sub>2</sub>, <sup>3</sup>J = 6.8 Hz), 2.07 (s, 3H, CH<sub>3</sub>C<sub>6</sub>H<sub>4</sub>CH(CH<sub>3</sub>)<sub>2</sub>), 2.71 (sept, 1H, CH<sub>3</sub>C<sub>6</sub>H<sub>4</sub>CH(CH<sub>3</sub>)<sub>2</sub>, <sup>3</sup>J = 6.8 Hz), 4.16 (s, 6H, NCH<sub>2</sub>P, PTA), 4.45 (s, 6H, NCH<sub>2</sub>N, PTA), 5.88 (d, 2H, CH<sub>3</sub>C<sub>6</sub>H<sub>4</sub>CH(CH<sub>3</sub>)<sub>2</sub>, <sup>3</sup>J = 6.4 Hz), 5.94 (d, 2H, CH<sub>3</sub>C<sub>6</sub>H<sub>4</sub>CH(CH<sub>3</sub>)<sub>2</sub>, <sup>3</sup>J = 6.4 Hz), 6.88 (s, 1H, CH of DBM), 7.54 (m, 4H, Ph of DBM), 7.63 (m, 2H, Ph of DBM), 8.00 (d, 4H, Ph of DBM, <sup>3</sup>J = 8.0 Hz). <sup>13</sup>C NMR (CD<sub>3</sub>CN, 293 K):  $\delta$  17.5 (s, CH<sub>3</sub>C<sub>6</sub>H<sub>4</sub>CH(CH<sub>3</sub>)<sub>2</sub>), 22.5 (s, CH<sub>3</sub>C<sub>6</sub>H<sub>4</sub>CH(CH<sub>3</sub>)<sub>2</sub>), 31.5 (s, CH<sub>3</sub>C<sub>6</sub>H<sub>4</sub>CH(CH<sub>3</sub>)<sub>2</sub>), 52.4 (d, PCH<sub>2</sub>N, PTA, J<sub>CP</sub> = 13.0 Hz), 73.4 (d, NCH<sub>2</sub>N, PTA, J<sub>CP</sub> = 7.7 Hz), 89.4, 90.7 (s, CH<sub>3</sub>C<sub>6</sub>H<sub>4</sub>CH(CH<sub>3</sub>)<sub>2</sub>), 96.7 (s, CH of DBM), 98.9, 105.8 (s, CH<sub>3</sub>C<sub>6</sub>H<sub>4</sub>CH(CH<sub>3</sub>)<sub>2</sub>), 128.5, 129.7, 133.2, 138.6 (s, Ph of DBM), 184.7 (s, C=O, DBM). <sup>31</sup>P NMR (CD<sub>3</sub>CN, 293 K):  $\delta$  -28.2 (s, PTA), -143.5 (sept, PF<sub>6</sub>, J<sub>PF</sub> = 706.4 Hz). ESI-MS (+) CH<sub>3</sub>OH (*m/z* (relative intensity, %)): 616 (100) [(*p*-cym)(RuDBM)(PTA)]<sup>+</sup>, 459 (5) [(*p*-cym)(RuDBM)]<sup>+</sup>.

### 2.2.6. [(hmb)Ru(DBM)(PTA)][SO<sub>3</sub>CF<sub>3</sub>][CHCl<sub>3</sub>] (6)

The synthesis was performed as for **4** using precursor **2** (yield 82%). **6** is soluble in alcohols, acetone, acetonitrile, chlorinated solvents, DMF and DMSO and slightly soluble in water. Mp: 248–250 °C. *Anal. Calc.* for C<sub>37</sub>H<sub>44</sub>Cl<sub>3</sub>F<sub>3</sub>N<sub>3</sub>O<sub>5</sub>PRuS: C, 38.61; H, 3.85; N, 3.65. Found: C, 38.57; H, 3.45; N, 3.36.  $\Lambda_M$  (CD<sub>3</sub>CN, 298 K, 10<sup>-4</sup> mol/L): 125 S cm<sup>2</sup> mol<sup>-1</sup>. IR (cm<sup>-1</sup>): 2926w  $\nu$ (C–H), 1589m, 1519vs  $\nu$ (C=O; C=C), 1475m, 1374s, 1260vs, 1148s, 1030vs  $\nu$ (SO<sub>3</sub>-CF<sub>3</sub>), 971s, 947vs, 722m, 636m. <sup>1</sup>H NMR (CD<sub>3</sub>CN, 293 K):  $\delta$  2.12 (s, 18H, CH<sub>3</sub>(hmb)), 4.07 (s, 6H, NCH<sub>2</sub>P, PTA), 4.39 (m, 6H, NCH<sub>2</sub>N, PTA), 6.89 (s, 1H, CH of DBM), 7.55 (m, 4H, Ph of DBM), 7.64 (m, 2H, Ph of DBM), 8.08 (d, 4H, Ph of DBM, <sup>3</sup>J = 8.0 Hz). <sup>13</sup>C NMR (CD<sub>3</sub>-CN, 293 K):  $\delta$  16.4 (s, CH<sub>3</sub>(hmb)), 50.5 (d, PCH<sub>2</sub>N, PTA, J<sub>CP</sub> = 12.2 Hz), 73.5 (d, NCH<sub>2</sub>N, PTA, J<sub>CP</sub> = 7.2 Hz), 96.2 (s, C<sub>6</sub>(hmb)), 99.6 (s, CH DBM), 128.3, 130.0, 133.2, 139.3 (s, Ph of DBM), 184.1 (s, C=O of DBM). <sup>31</sup>P NMR (CD<sub>3</sub>CN, 293 K):  $\delta$  -35.2 (s, PTA). ESI-MS (+) CH<sub>3</sub>OH (*m/z* (relative intensity, %)): 644 (100) [(hmb)Ru(DBM)(PTA)]<sup>+</sup>, 487 (15) [(hmb)Ru(DBM)]<sup>+</sup>.

### 2.2.7. [(hmb)Ru(DBM)(PTA)][PF<sub>6</sub>][CHCl<sub>3</sub>][H<sub>2</sub>O] (7)

The synthesis was performed as for **6** using AgPF<sub>6</sub> (yield 79%). **7** is soluble in alcohols, acetone, acetonitrile, chlorinated solvents, DMF and DMSO and slightly soluble in water. Mp: 184–185 °C. *Anal. Calc.* for C<sub>33</sub>H<sub>44</sub>Cl<sub>3</sub>F<sub>6</sub>N<sub>3</sub>O<sub>3</sub>P<sub>2</sub>Ru: C, 44.10; H, 4.79; N, 4.54. Found: C, 43.93; H, 4.69; N, 4.42.  $\Lambda_M$  (CD<sub>3</sub>CN, 298 K, 10<sup>-4</sup> mol/L): 138 S cm<sup>2</sup> mol<sup>-1</sup>. IR (cm<sup>-1</sup>): 2924w  $\nu$ (C–H), 1589m, 1519vs  $\nu$ (C=O; C=C), 1475m, 1374s, 1279m, 1242m, 1014m, 972s, 947s, 834vs  $\nu$ (PF<sub>6</sub>), 722s, 556s. <sup>1</sup>H NMR (CD<sub>3</sub>CN, 293 K):  $\delta$  2.12 (s, 18H, CH<sub>3</sub>(hmb)), 4.07 (s, 6H, NCH<sub>2</sub>P, PTA), 4.39 (s, 6H, NCH<sub>2</sub>N, PTA), 6.89 (s, 1H, CH of DBM), 7.56 (m, 4H, Ph of DBM), 7.63 (m, 2H, Ph of DBM), 8.07 (d, 4H, Ph of DBM, <sup>3</sup>J = 8.0 Hz). <sup>13</sup>C NMR (CD<sub>3</sub>CN, 293 K):  $\delta$  16.9 (s, CH<sub>3</sub>(hmb)), 51.1 (d, PCH<sub>2</sub>N, PTA, J<sub>CP</sub> = 12.2 Hz), 74.0 (d, NCH<sub>2</sub>N, PTA, J<sub>CP</sub> = 7.1 Hz), 96.7 (s, C<sub>6</sub>(hmb)), 100.1 (s, CH of DBM), 128.8, 130.5, 133.7, 139.9 (s, Ph of DBM), 184.6 (s, C=O of DBM). <sup>31</sup>P NMR (CD<sub>3</sub>CN, 293 K):  $\delta$  -35.3 (s, PTA), -143.5 (sept, PF<sub>6</sub>, J<sub>PF</sub> = 706.4 Hz). ESI-MS (+) CH<sub>3</sub>OH (*m/z* (relative intensity, %)): 644 (100) [(hmb)Ru(DBM)(PTA)]<sup>+</sup>, 487 (15) [(hmb)Ru(DBM)]<sup>+</sup>.

## 2.3. X-ray crystallography

Red crystals for **3–7** were mounted on a glass fibre and used for data collection on a Bruker D8 Venture with Photon detector

equipped with graphite monochromated Mo K $\alpha$  radiation ( $\lambda = 0.71073$  Å). The data reduction was performed with the APEX2 [28] software and corrected for absorption using SADABS [29]. Crystal structures were solved by direct methods using the SIR97 program [30] and refined by full-matrix least-squares on  $F^2$  including all reflections using anisotropic displacement parameters by means of the WINGX crystallographic package [31,32]. Generally, anisotropic temperature factors were assigned to all atoms except for hydrogen atoms, which are riding their parent atoms with an isotropic temperature factor arbitrarily chosen as 1.2 times that of the respective parent. It should be noted that all crystals undergo degradation when they are removed from the mother liquor which has a high impact on the quality of the data. Several crystals of compounds **3–7** were measured and the structures were solved from the best data we were able to collect. For this reason isotropic temperature factors were assigned to some non H atoms in the structures. Attempts to solve disorder problems with one (SO<sub>3</sub>CF<sub>3</sub>)- molecule and one chloroform solvent molecule failed in compounds **4** and **6**, respectively. Instead, a new set of  $F^2$  (*hkl*) values with the contribution from solvent molecules withdrawn was obtained by the SQUEEZE procedure implemented in PLATON-94 [33]. Final  $R(F)$ ,  $wR(F^2)$  and goodness of fit agreement factors, details on the data collection and analysis can be found in Table 1.

## 2.4. Luminescence measurement

A Varian Cary-Eclipse fluorescence spectrofluorometer was used to obtain the fluorescence spectra. The spectrofluorometer was equipped with a xenon discharge lamp (peak power equivalent to 75 kW), Czerny–Turner monochromators, and a R-928 photomultiplier tube which is red sensitive (even 900 nm) with manual or automatic voltage controlled using Cary Eclipse software for Windows 95/98/NT system. The photomultiplier detector voltage was 700 V and the instrument excitation and emission slits were set at 5 and 5 nm, respectively.

## 2.5. DNA interaction studies

Stock solutions of calf thymus DNA (ct-DNA) (Sigma–Aldrich) were prepared by dissolving the solid material overnight in 10 mM phosphate buffer pH 7.4 containing 5 mM NaCl at 4 °C. The solution of ct-DNA in phosphate buffer gave a ratio of UV absorbance at 260 and 280 nm,  $A_{260}/A_{280}$ , of ca. 1.9, indicating that the DNA was sufficiently free from protein. The concentration of ct-DNA solution was determined by UV absorbance at 260 nm. The molar absorption coefficient,  $\epsilon_{260}$ , was taken as 6600 M<sup>-1</sup> cm<sup>-1</sup> [34]. Complexes and ligands were dissolved in DMSO.

## 2.6. Electronic absorption titration

Electronic absorption spectra were carried out at 25 °C by fixing the concentration of the complex or ligands, with DNA concentration ranging from 0 to 35 10<sup>-6</sup> M. Absorption spectra were measured at 200–600 nm in 50 mM phosphate buffer pH 7.4. The complex solution was titrated with the DNA, and changes on the intensity of the bands of the complex were monitored. The intrinsic binding constant ( $K_b$ ) for the interaction of the complexes with ct-DNA was determined from a plot of  $[DNA]/(\epsilon_a - \epsilon_f)$  versus  $[DNA]$  using absorption spectral titration data and the following equation [35]:

$$\frac{[DNA]}{|\epsilon_a - \epsilon_f|} = \frac{[DNA]}{|\epsilon_b - \epsilon_f|} + \frac{1}{K_b |\epsilon_b - \epsilon_f|} \quad (1)$$

where  $[DNA]$  is the concentration of DNA, the apparent absorption coefficients  $\epsilon_a$ ,  $\epsilon_f$  and  $\epsilon_b$  correspond to  $A_{obsd}/[\text{complex}]$ , the

**Table 1**  
Crystallographic data and structural refinement details for 3–7.

Compound	3	4	5	6	7
Chemical formula	C <sub>21</sub> H <sub>17</sub> ClO <sub>2</sub> Ru	C <sub>32</sub> H <sub>37</sub> F <sub>3</sub> N <sub>3</sub> O <sub>5</sub> RuS	C <sub>31</sub> H <sub>37</sub> F <sub>6</sub> N <sub>3</sub> O <sub>2</sub> P <sub>2</sub> Ru	C <sub>37</sub> H <sub>44</sub> Cl <sub>6</sub> F <sub>3</sub> N <sub>3</sub> O <sub>5</sub> RuS	C <sub>34</sub> H <sub>44</sub> Cl <sub>3</sub> F <sub>6</sub> N <sub>3</sub> O <sub>3</sub> P <sub>2</sub> Ru
CCDC	1449967	1449968	1449969	1449970	1449966
M/gmol <sup>-1</sup>	437.86	764.74	760.64	1150.90	926.08
T (K)	100	100	100	100	100
λ (Å)	0.71073	0.71073	0.71073	0.71073	0.71073
Crystal system	monoclinic	orthorhombic	orthorhombic	monoclinic	monoclinic
Space group	P2 <sub>1</sub> /c	Pbca	Pbca	P2 <sub>1</sub> /c	P2 <sub>1</sub> /c
a (Å)	11.1175(9)	10.169(3)	10.0960(19)	9.1857(4)	9.5940(9)
b (Å)	11.6046(9)	21.587(6)	20.469(4)	24.3202(11)	36.361(5)
c (Å)	13.8839(10)	30.539(9)	30.285(5)	19.8960(8)	11.4295(11)
β (°)	104.575(3)	90	90	100.877(2)	97.265(4)
V (Å <sup>3</sup> )	1733.6(2)	6704(3)	6259(2)	4364.9(3)	3955.2(7)
Z	4	8	8	4	4
ρ (g cm <sup>-3</sup> )	1.678	1.515	1.615	1.751	1.555
μ (mm <sup>-1</sup> )	1.069	0.638	0.674	1.055	0.746
Unique reflections	6024	28956	38237	21909	12710
R <sub>int</sub>	0.055	0.096	0.149	0.116	0.088
Goodness-of-fit (GOF) on F <sup>2</sup>	1.011	0.962	1.262	1.055	1.098
R1 [I > 2σ(I)] <sup>a</sup>	0.035	0.051	0.133	0.092	0.089
wR2 [I > 2σ(I)] <sup>a</sup>	0.059	0.123	0.306	0.193	0.171

$$^a R(F) = \frac{\sum |F_o| - |F_c|}{\sum |F_o|}; wR(F^2) = [\sum w(F_o^2 - F_c^2)^2 / \sum wF_o^4]^{1/2}.$$

extinction coefficient for the free metal complex and the extinction coefficient for the metal complex in the fully bound form, respectively. The  $K_b$  value is given by the ratio of the slope to the intercept.

## 2.7. Competitive binding studies

### 2.7.1. Major groove displacement assay

A well-known major groove binder, ethidium bromide (EB), was used to perform the major groove displacement assays. The competitive binding experiment was carried out by maintaining the ethidium bromide (EB) and ct-DNA concentration at 5 μM and 55.7 μM, respectively, while increasing the concentration of different complexes. Fluorescence quenching spectra were recorded using a Hitachi 4500 spectrofluorimeter with an excitation wavelength of 490 nm and emission spectrum in the range 500–700 nm. The fluorescence decrease in the emission spectra was corrected according to Eq. (2):

$$F_c = F_m \times e^{\frac{(A_1 + A_2)}{2}} \quad (2)$$

where  $F_c$  and  $F_m$  are the corrected and measured fluorescence, respectively [36] and  $A_1$  and  $A_2$  are the absorbances of tested compounds at the exciting and emission wavelengths. For fluorescence quenching experiments, Stern–Volmer's Eq. (3) was used:

$$\frac{F_0}{F_c} = 1 + k_q \tau_0 [C] = 1 + K_{sv} [C] \quad (3)$$

where  $F_0$  and  $F_c$  represent the fluorescence intensity in the absence and presence of the metal complexes, respectively,  $[C]$  is the concentration of the complex and  $K_{sv}$  is the Stern–Volmer constant that can be obtained from fluorescence values plotted as  $F_0/F_c$  versus the complex concentration [36]. All experiments involving ct-DNA were performed at room temperature in phosphate buffer solution (50 mM, pH 7.4). The apparent binding constant ( $K_{app}$ ) of the metal complexes has been calculated by using the Eq. (4):

$$K_{EB}[EB] = K_{app}[C] \quad (4)$$

in which the complex concentration  $[C]$  is the value at a 50% reduction of the fluorescence intensity of EB and  $K_{EB} = 1.0 \times 10^7 \text{ M}^{-1}$  ( $[EB] = 5.0 \text{ μM}$ ) [37].

### 2.7.2. Minor groove displacement assay

A minor groove binders, 4',6-diamidino-2-phenylindole (DAPI), was used to perform the minor groove displacement assays. In a typical experiment, the changes in the emission spectra of DAPI complex with the DNA in 50 mM phosphate buffer pH 7.4, were monitored upon addition of increasing concentrations of compounds at room temperature. Fluorescence quenching data were evaluated after excitation of DAPI-ct-DNA complex at 338 nm and recording the spectra from 400 to 600 nm. Values of  $K_{sv}$  constants were evaluated by using Eq. (3), after that all quenching fluorescence values obtained were corrected according to the Eq. (2). In the presence of enhancement of fluorescent, the values of  $K_{sv}$  were evaluated as previously described [38,39].

## 2.8. BSA binding studies

The protein-binding study was performed by tryptophan fluorescence quenching experiments using bovine serum albumin (BSA). Bovine serum albumin (Sigma–Aldrich) stock solutions were prepared in 50 mM potassium phosphate buffer at pH 7.4. Fluorescence measurements were carried out with a Hitachi 4500 spectrofluorimeter by keeping the concentration of BSA constant ( $15 \times 10^{-6} \text{ M}$ ) while varying the complex concentration from were added to protein solution from 0 to  $40 \times 10^{-6} \text{ M}$ , at room temperatures. Fluorescence intensities were recorded after each successive addition of complex solution and equilibration (ca. 5 min). Fluorescence spectra were recorded from 300 to 450 nm at an excitation wavelength of 285 nm. The values of Stern Volmer constant  $K_{sv}$  and the bimolecular quenching rate constant  $K_q$  of the metal complexes to BSA were evaluated following the Eq. (3) considering that  $\tau_0$  was the average fluorescence lifetime of the fluorophore in the absence of drug with a value of  $10^{-8} \text{ s}$  [37]. All fluorescent values were corrected by Eq. (2).

Considering the existence of similar and independent binding sites in the BSA for the static quenching interaction, the binding constant ( $K_b$ ) and the number of the binding sites ( $n$ ) for the different complexes on BSA can be estimated using the Scatchard Eq. (5): [40,41]

$$\frac{\left(\frac{F_0 - F_c}{F_0}\right)}{[C]} = nK_b - K_b \left(\frac{F_0 - F_c}{F_0}\right) \quad (5)$$

where  $n$  is the number of binding sites for protein,  $K_b$  ( $M^{-1}$ ) is the association binding constant that can be calculated from the slope of plot of  $((F_0 - F_C)/F_0)/[C]$  versus  $((F_0 - F_C)/F_0)$ ,  $n$  is given by the ratio of the y intercept to the slope.

## 2.9. Cell culture and inhibition of cell growth

### 2.9.1. Cells

RPMI8226 (RPMI) and U266 MM cell lines (purchased from ATCC, LGC Standards, Milan, IT). Cell authentication was performed by IST (Genova, Italy). Cell lines were cultured in RPMI medium (Lonza, Milan, IT) supplemented with 10% fetal bovine serum (FBS), 2 mM L-glutamine, 100 IU/ml penicillin, 100  $\mu$ g streptomycin and 1 mM sodium pyruvate. Cell lines were maintained at 37 °C with 5% CO<sub>2</sub> and 95% humidity.

### 2.9.2. MTT assay

$3 \times 10^3$  cells/well were seeded in 96-well plates, in a final volume of 100  $\mu$ L. After 1 incubation day, DBM complexes or vehicle were added and cell viability was evaluated up to 72 h. Four replicate wells were used for each treatment. At the indicated time point, cell viability was assessed by adding 0.8 mg/ml of MTT (Sigma–Aldrich) to the media. After 3 h, the plates were centrifuged, the supernatant was discharged, and the pellet was solubilized with 100  $\mu$ L/well DMSO. The absorbance of the samples against a background control (medium alone) was measured at 570 nm using an ELISA reader microtiter plate (BioTek Instruments, Winooski, VT).

### 2.9.3. Cell cycle analysis

$3 \times 10^4$  cells/ml were incubated with 25  $\mu$ M of the DBM complexes, for 48 h. Then, cells were fixed for 1 h by adding ice-cold 70% ethanol and washed with staining buffer (PBS, 2% FBS and 0.01% NaN<sub>3</sub>). Next, the cells were treated with 10  $\mu$ g/ml ribonuclease A solution (Sigma–Aldrich), incubated for 30 min at 37 °C, stained for 30 min at room temperature with 20  $\mu$ g/ml of propidium iodide (Sigma–Aldrich) and finally analyzed by flow cytometry using linear amplification.

### 2.9.4. Apoptosis assays

The exposure of phosphatidylserine on MM cells was detected by Annexin V staining and cytofluorimetric analysis. Briefly,  $3 \times 10^4$ /ml cells were treated with 25  $\mu$ M of the appropriate drugs for 72 h. Four replicates were used for each treatment. After treatment, the cells were stained with 5  $\mu$ L of Annexin V FITC (Vinci Biochem, Vinci, Italy) for 10 min at room temperature, washed once with binding buffer (10 mM HEPES/NaOH, pH 7.4, 140 mM NaCl, 2.5 mM CaCl<sub>2</sub>) and analyzed on a FACScan flow cytometer using CellQuest software.

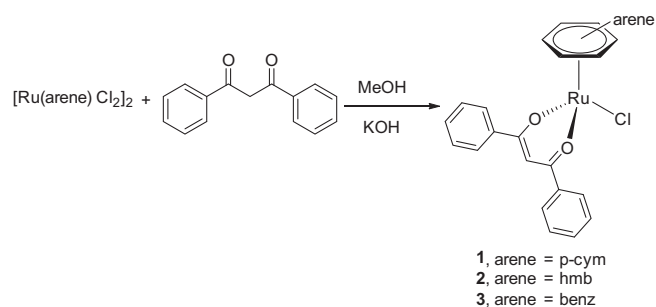
### 2.9.5. Statistical analysis

The data presented represent the mean and standard deviation (SD) of at least 3 independent experiments. The statistical significance was determined by Student's *t*-test; \*, #, §*p* < 0.01. The statistical analysis of IC<sub>50</sub> levels was performed using Prism 5.0a (Graph Pad).

## 3. Results and discussion

### 3.1. Synthesis and characterization

The arene-Ru(II) complexes **1–3** were prepared in high yield in a single step (Scheme 1), by interaction of [(arene)RuCl<sub>2</sub>]<sub>2</sub> (arene = *p*-cymene (*p*-cym), hexamethylbenzene (hmb) and benzene(benz)) with dibenzoylmethane DBMH in basic solution.

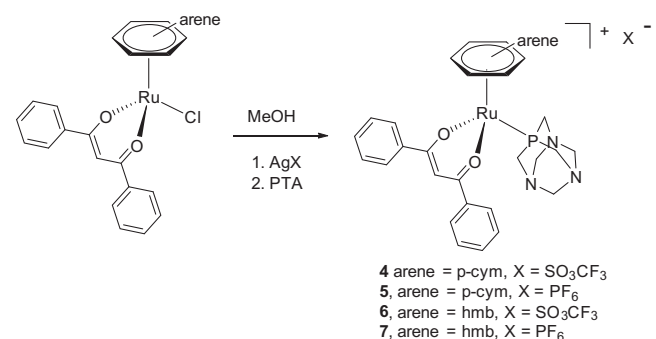


**Scheme 1.** Synthesis of complexes **1–3**.

By substitution of chloride ligand with PTA in the ruthenium coordination environment, achieved by adding PTA and silver salts, i.e. AgX where X = SO<sub>3</sub>CF<sub>3</sub> or PF<sub>6</sub>, cationic complexes **4–7** were isolated (Scheme 2). Complexes **1–7** are air stable and soluble in alcohols, acetone, acetonitrile and DMSO and chlorinated solvents but cationic complexes **4–7** are also partially soluble in water. The IR spectra of **1–7** display the typical shift of  $\nu(C=O)$  of  $\beta$ -diketones after metal coordination [42,43]. For complexes **1–3** also the  $\nu(Ru-Cl)$  has been detected in the far-IR region. By contrast, the IR spectra of **5** and **7** display a strong, sharp absorption at 825 and 826  $cm^{-1}$  due to the PF<sub>6</sub> counteranion [44,45] whereas the spectra of **4** and **6** contain a characteristic absorption pattern in the region 1000–1200  $cm^{-1}$ , typical of a not-coordinated O<sub>3</sub>SCF<sub>3</sub> anion [46]. The <sup>1</sup>H NMR spectra of **1–7** display all the expected signals due to the coordinated arene rings, DBM ligand and for **4–7** also of PTA. The resonances due to the PTA ligand are shifted to lower field with respect to those of uncoordinated PTA confirming its coordination to the ruthenium center [47]. The <sup>31</sup>P NMR spectra of **4** and **5**, containing the *p*-cymene moiety, display a singlet centered at ca. –28 ppm due to PTA, whereas **6** and **7** with the hexamethyl moiety show the PTA resonance at ca. –35 ppm, in a range typical of related compounds and in accordance with the existence of only one species in solution [48].

The ESI mass spectra of **1–3** show a main peak corresponding to [Ru(arene)(DBM)]<sup>+</sup> fragment. Whereas the ESI mass spectra of **4–7** show two main peak envelopes, that of highest relative intensity corresponding to the intact [Ru(arene)(DBM)(PTA)]<sup>+</sup> species, the other being due to the [Ru(arene)(DBM)]<sup>+</sup> fragment formed upon PTA dissociation. For complexes **1–3**, conductivity measurements in acetonitrile indicate a slight dissociation of the chloride at room temperature. Whereas, in acetonitrile, ionic derivatives **4–7** display conductivity values within the range typical of 1:1 electrolytes [49].

The stability of **6** (the most cytotoxic compound, see Section 3.4) was also determined under pseudo-pharmacological conditions in 5 mM NaCl solution (being a model for the low intracellular



**Scheme 2.** Synthesis of complexes **4–7**.

chloride concentration in cells) and in 100 mM NaCl solution (approximating to the higher chloride levels in blood). Solutions of the complexes ( $c = 2.0$  mM) in aqueous NaCl ( $c = 5$  mM or 100 mM in  $D_2O$  containing 10% of  $[D_6]DMSO$ ) were prepared and maintained at  $37^\circ C$  for 7 days. The decomposition of the complexes was monitored by  $^1H$  and  $^{31}P$  NMR spectroscopy. The complex  $[(hmb)Ru(DBM)(PTA)][SO_3CF_3]$  did not undergo hydrolysis in either 5 and 100 mM NaCl solutions, i.e. the  $^1H$  and  $^{31}P$  NMR spectra of **6** remained unchanged after 7 days (see Fig. 1).

### 3.2. Crystal structures

The solid state structures of **3–7** were established by X-ray crystallography (see Section 2). Their structures are shown in Figs. 2–6 and principal bond parameters are given in the Table S1. In general, the structures consist in “piano stool” distribution formed by the ruthenium-arene unit bound to the chloride, PTA and DBM ligand. The distances of ruthenium atom and arene rings are 1.650, 1.700, 1.705, 1.710 and 1.695 Å for compounds **3**, **4**, **5**, **6** and **7**, respectively, in good agreement with others published distances [50,51]. Compound **3** crystallizes in  $P2_1/c$  monoclinic group. In mononuclear complex, the metal is coordinated with a pseudo-octahedral geometry to one benzene, formally occupying three contiguous coordination positions, one chloride atom and two positions corresponding to one DBM ligand (Fig. 2). The Ru–Cl distance has a value of 2.425(1) Å while DBM coordinates in a chelate mode with Ru–O bond distances of 2.055(3) and 2.068(3) Å. The chloride atom and DBM molecule occupy a *fac* disposition with angles in the range 84.03(8)–88.34(11). These mononuclear units present *staking* interactions (3.597 Å) between the arene and one of the benzene pertaining to DBM of a neighboring molecule.

Compound **4** crystallizes in  $Pbca$  orthorhombic group. In this case, coordination geometry about the metal center ruthenium like those in **3**, is typical “piano stool” with one position occupied by phosphorous atom from PTA, two oxygen atoms from DBM ligand and arene ring in  $\eta^6$ -manner. The Ru–P distance has a value of 2.3140(17) Å while DBM coordinates in a quelate mode with Ru–O bond distances of 2.071(4) and 2.078(4) Å. The phosphorous atom and DBM molecule occupy a *fac* disposition with angles in the

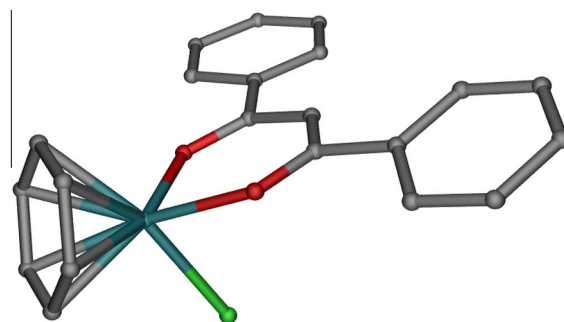


Fig. 2. Perspective view of **3** [(benz)RuCl(DBM)]. Hydrogen atoms have been omitted for clarity.

range 86.11(11)–88.26(15). In this molecule, planes containing benzene rings pertaining to DBM ligand present a dihedral angle of  $37.63^\circ$ . These mononuclear compounds present partial *staking* interactions (3.440 Å) between the arene rings of neighboring molecules due to the steric impediments of methyl groups. Compound **5** crystallizes in  $Pbca$  orthorhombic group. In this case, coordination geometry about the metal center ruthenium is similar to **4**. One position is occupied by phosphorous atom from PTA and the others two positions have oxygen atoms from DBM ligand. The principal different of this compound with **4** is the presence of  $(PF_6)^-$  anion instead  $(SO_3CF_3)^-$ .

The Ru–P distance has a value of 2.302(7) Å while DBM coordinates in a chelate mode with Ru–O bond distances of 2.061(15) and 2.067(15) Å. The phosphorous atom and DBM molecule occupies a *fac* disposition with angles in the range 86.0(5)–89.0(5). In this molecule, planes containing benzene rings pertaining to DBM ligand present a dihedral angle of  $34.53^\circ$ . These mononuclear compounds present partial *staking* interactions (3.351 Å) between the arene rings due to the steric impediments of methyl groups.

Compound **6** crystallizes in  $P2_1/c$  monoclinic group. In this case, coordination geometry about the metal center ruthenium like those in the above compounds, with one position occupied by phosphorous atom from PTA, two oxygen atoms from DBM ligand

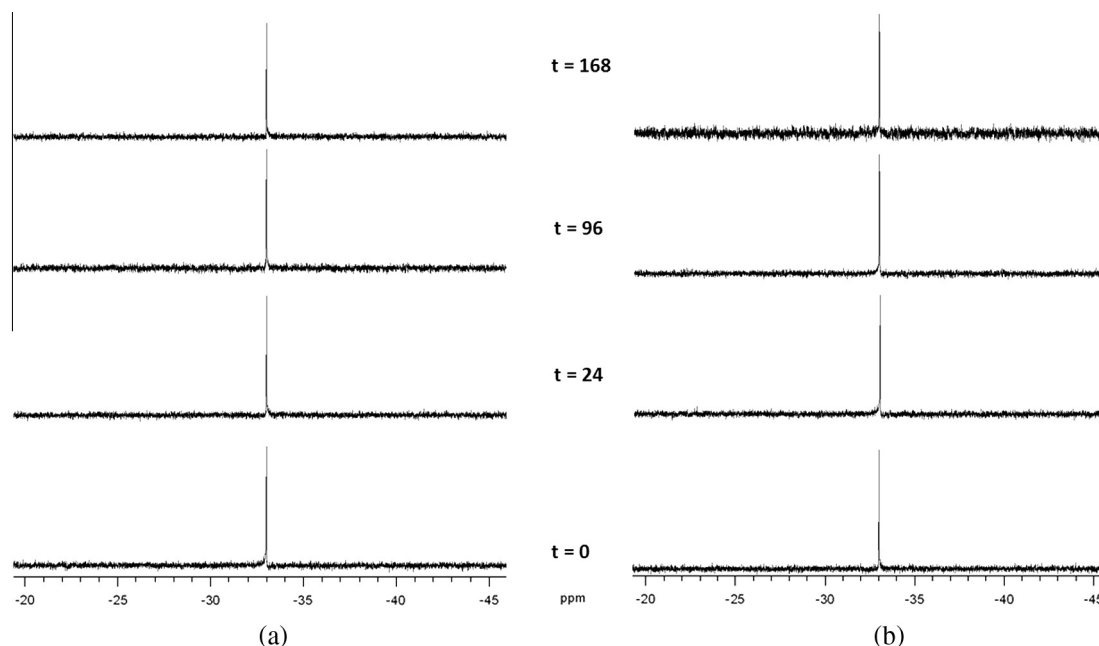
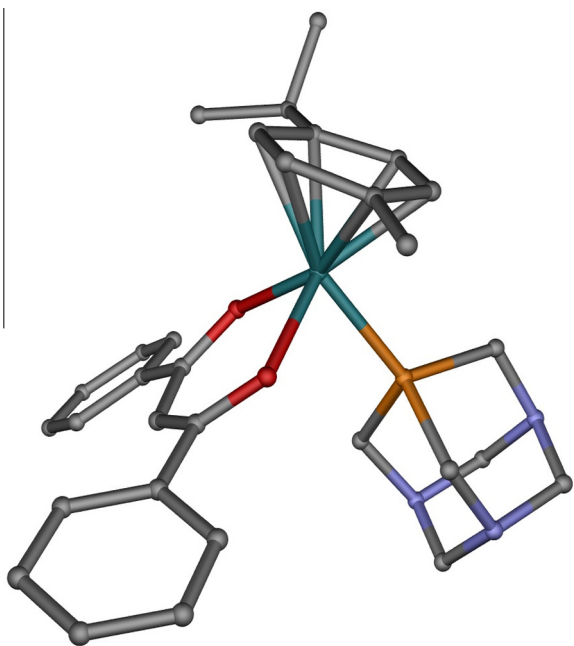
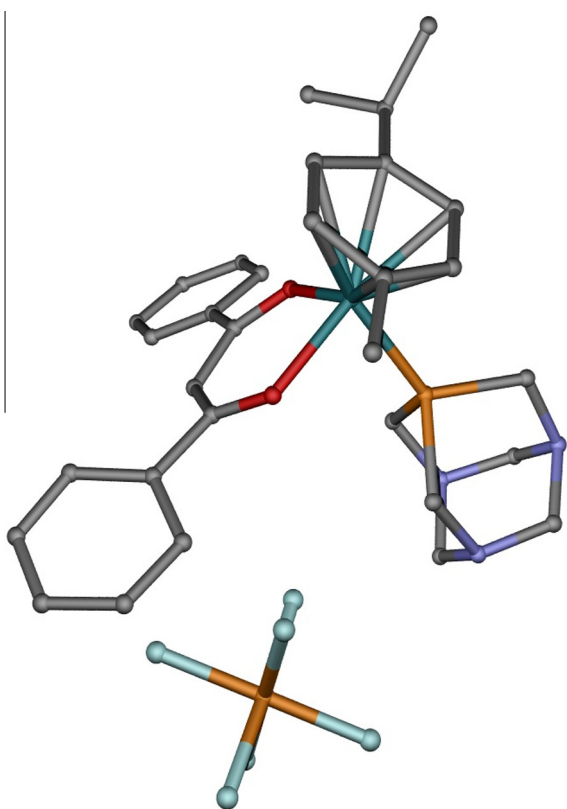


Fig. 1.  $^{31}P$  NMR spectra of **6** in 5 mM (a) and in 100 mM (b) aqueous NaCl solution.



**Fig. 3.** View of **4** [(p-cym)Ru(DBM)(PTA)](SO<sub>3</sub>CF<sub>3</sub>). Anion and hydrogen atoms have been omitted for clarity.



**Fig. 4.** View of complex **5** [(cym)Ru(DBM)(PTA)](PF<sub>6</sub>). Hydrogen atoms have been omitted for clarity.

and hexamethylbenzene in η<sup>6</sup>-manner. This mononuclear compound contains one (SO<sub>3</sub>CF<sub>3</sub>)<sup>−</sup> anion and three chloroform solvent molecules. The Ru–P distance has a value of 2.297(3) Å while DBM coordinates in a chelate mode with Ru–O bond distances of 2.073(6) and 2.079(6) Å. The phosphorous atom and DBM molecule

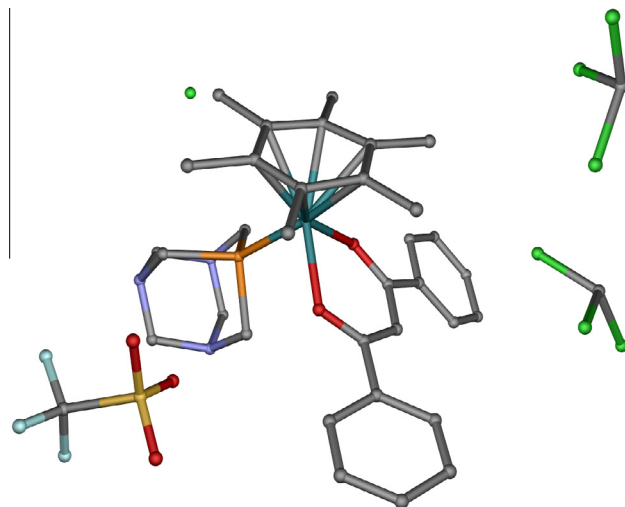


**Fig. 5.** View of **6** [(hmb)Ru(DBM)(PTA)](SO<sub>3</sub>CF<sub>3</sub>)(CHCl<sub>3</sub>)<sub>3</sub>. One chloroform solvent molecule and hydrogen atoms have been omitted for clarity.

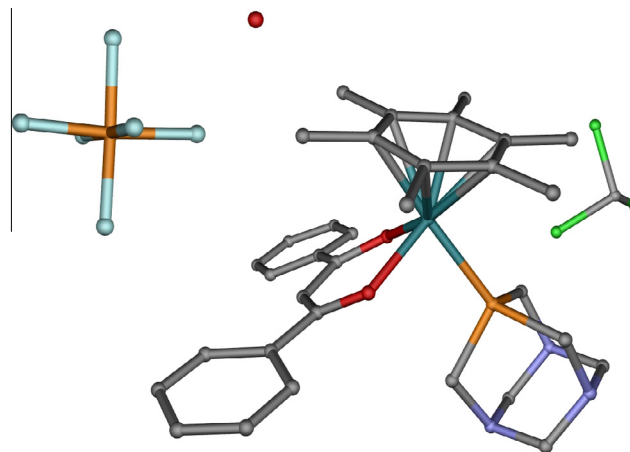


**Fig. 6.** View of **7** [(hmb)Ru(DBM)(PTA)](PF<sub>6</sub>)(CHCl<sub>3</sub>)<sub>3</sub>[H<sub>2</sub>O]. Hydrogen atoms have been omitted for clarity.

occupies a *fac* disposition with angles in the range 81.40(19)–88.12(19). In this molecule, planes containing benzene rings pertaining to DBM ligand present a dihedral angle of 35.67°. These mononuclear compounds present staking interactions (3.314 Å) between the arene and one of the benzene pertaining to DBM of a neighbouring molecule.

Compound **7** crystallizes in *P*2<sub>1</sub>/*c* monoclinic group. In this case, coordination geometry about the metal center ruthenium like those in **6**. One position is occupied by phosphorous atom from PTA and the others two positions have oxygen atoms from DBM ligand. The principal different of this compound with **6** is the presence of (PF<sub>6</sub>)<sup>−</sup> anions and crystallization water molecules. The Ru–P distance has a value of 2.336(3) Å and DBM coordinates in a chelate mode with Ru–O bond distances of 2.055(8) and 2.096(7) Å. The phosphorous atom and DBM molecule occupies a *fac* disposition with angles in the range 82.8(2)–87.1(2). In this molecule, planes containing benzene rings pertaining to DBM ligand present a dihedral angle of 35.67°. These mononuclear compounds present *steking* interactions (3.379 Å) between the arene and one of the benzene pertaining to DBM of a neighboring molecule. There is a strong hydrogen bond (2.911 Å) between the water molecule and the nitrogen atom N3B pertaining to the PTA ligand.

### 3.3. Luminescence studies

Due to its extended aromaticity, the DBMH ligand is a good candidate for enhanced emissive properties. For this reason, room temperature solid state emission spectra of the synthesized compounds **1–7** have been recorded. As previously reported [52], coordination compounds based on dibenzoylmethane ligand exhibit broad emission bands with the maxima peaking around 350 nm, respectively. When excited at 310 nm, the main emissions of compounds **1–7** (Fig. 7) are slightly shifted to 360 and 375 nm compared to the DBMH ligand.

The similarity of the emission spectra of **1–7** is in agreement with the explanation, which indicates that ligand centred  $\pi-\pi^*$  excitation is responsible for the emission. On the other hand, it can be presumed that all these emissions originate from  $\pi^* \rightarrow$  or even  $\pi^* \rightarrow \pi$  transitions in which the energy gap slightly decreases (red shift or bathochromic emission) according to the coordination of the ligands to metal centres due to the increased rigidity provided to the system [53].

### 3.4. Biological studies

#### 3.4.1. Cytotoxicity

U266 and RPMI human multiple myeloma cell lines were resistant to a 48 h exposure to cisplatin at 1  $\mu\text{g}/\text{mL}$ , as recently described by Gougelet [54]. The ability of **1–7**, used at different doses (1–500  $\mu\text{M}$ ) and incubation times (from 24 up to 72 h), to affect the viability of U266 and RPMI human multiple myeloma cells, has been evaluated by MTT assay. As shown in Table 2, all ruthenium derivatives were effective in reducing the viability of both MM cells, in a time- and dose-dependent manner starting from 24 h post-treatments (Figs. S1 and S2, Supporting information).

$\text{IC}_{50}$  values, calculated at 72 h post-treatments, indicate different efficacy of DBM complexes in reducing cell viability. All complexes are comparatively more effective than the free neutral DBMH proligand. Among the similar chloride species **1–3**, compound **3**, containing benzene on Ru, is the less effective toward both tumour cell lines while **1** with *p*-cymene on Ru displays the highest efficacy. Previous studies from Sadler and Dyson on *p*-cymene-Ru  $\beta$ -diketonates against the A2780 cell line, reported that the introduction of PTA on the complex increased their activity [23,24], here we observe a reduction of the efficacy for complex **4** and **5** with respect to neutral complex **1**. The hmb-Ru(II) complex **2** is slightly less active than *p*-cym-Ru(II) **1**. In the case of ionic hmb complexes **6** and **7**, compared to **2**, we observe an increase and a reduction of activity, respectively. The  $\text{SO}_3\text{CF}_3^-$  counterion seems to improve the activity in **4** and **6**, with respect to  $\text{PF}_6^-$  in **5** and **7**.

The reduced cell viability effect, observed with DBM complexes, was evaluated by investigating their effect on cell cycle regulation

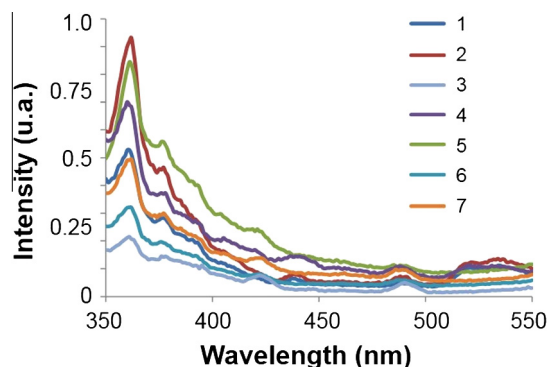


Fig. 7. The experimental emission spectra of compounds **1–7** after excitation at 310 nm in solid state at room temperature.

Table 2

DBM complexes reduce cell viability in U266 and RPMI human multiple myeloma (MM) cell lines. U266 and RPMI cell lines, were cultured up to 72 h with different doses (0–500  $\mu\text{M}$ ) of DBM complexes. Cell viability was determined by MTT assay. Data shown are expressed as mean  $\pm$  SE of three separate experiments.  $\text{IC}_{50}$  values were calculated using Prism 5.0, at 72 h post-treatments.

Compound	RPMI ( $\text{IC}_{50}$ $\mu\text{M}$ ) $\pm$ S.E.	U266 ( $\text{IC}_{50}$ $\mu\text{M}$ ) $\pm$ S.E.
<b>1</b>	16.9 $\pm$ 0.2	16.6 $\pm$ 0.1
<b>2</b>	19.8 $\pm$ 0.6	20.1 $\pm$ 1.6
<b>3</b>	37.8 $\pm$ 1.8	39.2 $\pm$ 2.7
<b>4</b>	20.2 $\pm$ 1.8	19.4 $\pm$ 0.6
<b>5</b>	21.3 $\pm$ 1.7	23.1 $\pm$ 1.2
<b>6</b>	16.7 $\pm$ 1.7	15.5 $\pm$ 1.1
<b>7</b>	40.2 $\pm$ 2.5	38.4 $\pm$ 3.1
<b>DBMH</b>	463.2 $\pm$ 12	448.2 $\pm$ 18.2

and/or on cell death induction, in MM cell lines. First, the effects of DBM complexes (at 25  $\mu\text{M}$  dose), on cell cycle phases, was analyzed at 24 and 48 h post-treatments: while at 24 h no effects were observed (results not shown), at 48 h post-treatments an effect on cell cycle phases was demonstrated. In fact, we found that all the DBM complexes induce an accumulation in G1 and in Sub-G1 (indicating DNA fragmentation) phases of cell cycle compared with vehicle, with **5** showing the higher percentage of Sub-G1 and G1 cell accumulation (Fig. S3, Supporting information). Similar results were obtained in both MM cell lines. These results indicate that complexes **1–7** are able to induce cell cycle arrest and to increase the percentage of cells in sub-G1 phase, suggesting that DBM-treated cells activated a mechanism of cell death.

To further investigate the Sub-G1 cells status, after DBM complexes treatments we stained DBM-treated MM cell lines with Annexin-V and apoptotic cells death was determined. As shown (Fig. S4, Supporting information) DBM complexes are able to induce, with different percentage, apoptotic cell death with similar effects in both MM cell lines.

#### 3.4.2. Antioxidant activity

The in vitro antioxidant activities for the proligand DBMH and complexes **1–7** were determined by the DPPH assay [55,56] and results are given in Table 3.

Complexes **1–5** present higher scavenging activity against DPPH, compared to the DBMH proligand and **1**, **3** and **5** are also more efficient than Trolox used as control, while **6** and **7** show a much lower efficacy. Among the neutral complexes **1–3**, that containing the benzene moiety displays the highest antioxidant activity. The introduction of PTA decreases the antioxidant activity in all type of complexes, with a strong effect for hmb-Ru complexes **6** and **7**.

### 3.5. DNA-binding properties

#### 3.5.1. Electronic absorption titration

The interaction of proligand DBMH and complexes **1–7** with ct-DNA was followed by spectrophotometric titrations. In absence of ct-DNA, UV-Vis spectra of all compounds display intense bands around 240–280 and 300–350 nm (see Supplementary material,

Table 3

Antioxidant activity of DBMH and complexes **1–7**.

Compound	DPPH $\text{IC}_{50}$ $10^{-6}$ M
<b>1</b>	15.85 ( $\pm$ 0.20)
<b>2</b>	40.12 ( $\pm$ 0.80)
<b>3</b>	6.48 ( $\pm$ 0.10)
<b>4</b>	50.64 ( $\pm$ 0.29)
<b>5</b>	19.14 ( $\pm$ 0.10)
<b>6</b>	439.39 ( $\pm$ 7.25)
<b>7</b>	293.09 ( $\pm$ 5.18)
<b>DBMH</b>	155.52 ( $\pm$ 3.10)
<b>Trolox</b>	21.80 ( $\pm$ 0.80)

Fig. S5) due to the phenyl groups of DBM scaffold, and a medium intensity band close to 400 nm arising from a metal to ligand charge transfer transition, typical of these  $d^6$  arene-Ru(II) complexes [57]. From the absorption titration spectrum (Fig. S5, Supporting information) it is apparent that upon addition of ct-DNA to fixed concentrations of complexes 1–7 and DBMH, the intra ligand band (251 nm) displayed hyperchromism along with a negligible red shift. On the other hand bands in the range 300–350 nm exhibit hypochromism without any significant shift. The presence of isosbestic points in the titration curve indicate the presence of more than two species in the medium. To compare the binding affinity of the complexes with ct-DNA, the equilibrium binding constants ( $K_b$ ) have been evaluated and data reported in Table 4: a rather strong binding of DBMH, 4 and 6 to ct-DNA has been found. Among the neutral complexes 1–3 the one containing the hmb moiety (2) displays the greater affinity for ct-DNA. The introduction of PTA in ionic compounds with  $SO_3CF_3^-$  counterion (complexes 4 and 6) strongly increases the affinity for ct-DNA with respect to the other ionic complexes 5 and 7 with the  $PF_6^-$  counterion.

### 3.5.2. Competitive binding studies

In order to provide further evidence for the interaction mode of 1–7 with ct-DNA, EtBr displacement experiments have been performed by competitive binding fluorescence assay. The displacement of EtBr from the major groove of ct-DNA by a metal complex leads to a decrease in the fluorescence intensity. Quenching parameters for all compounds,  $K_s$  and  $K_{app}$  are reported in Table 4.

By addition of increasing amounts of complexes 1–7 and DBMH, the fluorescence spectra display a decrease of intensity of the emission band at 590 nm due to the EB-ct-DNA system (Fig. S6, Supporting information), thus indicating the displacement of EB from the major groove of the ct-DNA. The compound 2 with hmb moiety shows higher activity with respect to *p*-cymene and benzene derivatives 1 and 3 respectively. Among the ionic derivatives, 4 and 6 containing the  $SO_3CF_3^-$  counterion display lower binding activity with respect to  $PF_6^-$  derivatives 5 and 7. Further evidence for the interaction mode of DBMH and complexes 1–7 to ct-DNA was evaluated by using a displacement assay with DAPI [58]. All complexes show good binding affinity for the minor groove of DNA (Fig. S7, Supporting information). In more detail, all complexes are less effective than the free DBMH proligand and among the neutral complexes 1–3, the one containing the *p*-cymene moiety (1) is slightly more effective. Lower differences have been observed for ionic complexes 4–7. From the observed quenching binding parameters we can hypothesize that all complexes bind to DNA via intercalation mode with more affinity for the minor groove.

### 3.6. Protein binding studies

To understand the mechanism of interaction of 1–7 and DBMH with Bovine Serum Albumin (BSA), fluorescence quenching experiments have been carried out. The effect of complexes 1–7 and DBMH

**Table 4**  
Binding constant ( $K_b$ ), Stern–Volmer constant ( $K_{sv}$ ) and the apparent binding constant ( $K_{app}$ ) for DBMH complexes 1–7 for ct-DNA and EB-ct-DNA, DAPI-ct-DNA complexes.

Complex	ct-DNA	EB-ct-DNA		DAPI-ct-DNA
	$K_b$ $10^4$ M <sup>-1</sup>	$K_{sv}$ $10^4$ M <sup>-1</sup>	$K_{app}$ $10^5$ M <sup>-1</sup>	$K_{sv}$ $10^4$ M <sup>-1</sup>
1	3.59 (±0.09)	0.56 (±0.02)	2.80 (±0.10)	1.86 (±0.09)
2	4.99 (±0.10)	0.66 (±0.05)	3.30 (±0.25)	0.56 (±0.01)
3	2.86 (±0.10)	0.47 (±0.01)	0.85 (±0.05)	0.91 (±0.02)
4	11.48 (±0.15)	0.48 (±0.03)	2.40 (±0.15)	1.26 (±0.02)
5	3.82 (±0.10)	0.63 (±0.04)	3.15 (±0.20)	1.08 (±0.03)
6	17.91 (±0.23)	0.17 (±0.01)	0.85 (±0.05)	1.48 (±0.02)
7	2.55 (±0.39)	0.60 (±0.05)	3.00 (±0.25)	1.47 (±0.05)
DBMH	9.37 (±0.19)	0.20 (±0.06)	1.00 (±0.30)	2.84 (±0.13)

**Table 5**

Protein quenching constant ( $K_{sv}$ ), binding constant ( $K_b$ ), and number of binding sites ( $n$ ) for the interaction of DBMH and complexes 1–7 with BSA.

Complex	BSA binding			
	$K_{sv}$ $10^5$ M <sup>-1</sup>	$k_q$ $10^{12}$ M <sup>-1</sup> s <sup>-1</sup>	$K_b$ $10^5$ M <sup>-1</sup> s <sup>-1</sup>	$n$
1	1.22 (±0.07)	12.2 (±0.3)	0.61 (0.04)	1.23
2	0.53 (±0.03)	5.3 (±0.3)	0.52 (0.07)	1.01
3	0.62 (±0.04)	6.2 (±0.4)	0.38 (0.05)	1.21
4	0.70 (±0.01)	7.0 (±0.1)	0.19 (0.03)	1.65
5	0.55 (±0.02)	5.5 (±0.2)	0.25 (0.02)	1.40
6	0.49 (±0.01)	4.9 (±0.1)	0.24 (0.03)	1.51
7	0.21 (±0.02)	2.1 (±0.2)	0.17 (0.02)	1.14
DBMH	0.07 (±0.01)	0.7 (±0.1)	0.02 (0.00)	1.25

on BSA fluorescence intensity is shown in Fig. S8 (Supporting information). The strong fluorescence emission peak at 346 nm of BSA decreased when it was titrated with different amounts of 1–7. From the value of  $K_{sv}$  it appears that all complexes show more affinity for the protein with respect to DBMH proligand. Neutral complexes 1–3 are more active than their ionic derivatives and all the compounds containing the *p*-cymene moiety show a higher binding affinity to BSA than the others. The value of bimolecular quenching constant ( $k_q$ ), reported in Table 5 for all tested compounds, falls in the range 0.7–12.2  $10^{12}$  L mol<sup>-1</sup> s<sup>-1</sup>, which is higher than the maximum possible value for dynamic quenching (2.0  $10^{10}$  L mol<sup>-1</sup> s<sup>-1</sup>) [50]. These results might indicate that the quenching could be initiated not by dynamic collision but through the formation of the complex between quencher and fluorophore suggesting the involvement of a static quenching mechanism. The data of the binding constant ( $K_b$ ) together with the number of the binding sites ( $n$ ) that were found close to 1, suggest that there is only one binding site for these compounds on the BSA molecule.

## 4. Conclusions

A series of neutral ruthenium(II) arene complexes with dibenzoylmethane and their ionic derivatives embedding PTA and different counterions have been synthesized. The complexes were fully characterized by analytical and spectroscopic methods and the solid-state structures of neutral and ionic complexes have been determined by single-crystal X-ray diffraction. The stability under pseudo-physiological conditions was also investigated for the most cytotoxic complex (6) showing that it is stable in these environments up to seven days. All physicochemical techniques tested demonstrated that all the compounds effectively bind with DNA through intercalative/electrostatic interactions with higher binding affinity through minor DNA groove.

The protein binding properties of the compounds suggest that they interact with protein (BSA) and the binding affinity increases in all complexes with an affinity from 3 to 15-fold higher to that reported for the free DBMH ligand. The higher antioxidant activity of complexes 1, 3 and 5 with respect to Trolox suggests a possible application of these compounds in the elimination of the hydroxyl radical. All compounds reported here possess a good cytotoxicity toward both U266 and RPMI human multiple myeloma cell lines. In the case of ionic complexes, the  $SO_3CF_3^-$  counterion increases the in vitro anticancer activity with respect to  $PF_6^-$ . In conclusion the coordination of dibenzoylmethane to the arene-ruthenium(II) moiety is able to preserve the interaction with DNA, but increases the binding to BSA, the free radical scavenger properties and the cytotoxicity towards tumor cell lines.

## Author contributions

The manuscript was written through contributions of all authors. All authors have given approval to the final version of the manuscript.

## Notes

The authors declare no competing financial interest.

## Acknowledgments

We thank the University of Camerino for financial support.

## Appendix A. Supplementary material

CCDC 1449966–1449970 contains the supplementary crystallographic data for this paper. These data can be obtained free of charge from The Cambridge Crystallographic Data Centre via [www.ccdc.cam.ac.uk/data\\_request/cif](http://www.ccdc.cam.ac.uk/data_request/cif). Supplementary data associated with this article can be found, in the online version, at <http://dx.doi.org/10.1016/j.ica.2016.04.031>.

## References

- [1] A.A. Nazarov, C.G. Hartinger, P.J. Dyson, *J. Organomet. Chem.* 751 (2014) 251.
- [2] Y.K. Yan, M. Melchart, A. Habtemariam, P.J. Sadler, *Chem. Commun.* (2005) 4764. DOI 10.1039/b508531b.
- [3] A. Martínez, C.S.K. Rajapakse, R.A. Sánchez-Delgado, A. Varela-Ramirez, C. Lema, R.J. Aguilera, *J. Inorg. Biochem.* 104 (2010) 967.
- [4] E. Corral, A.C.G. Hotze, H. Den Dulk, A. Leczkowska, A. Rodger, M.J. Hannon, J. Reedijk, *J. Biol. Inorg. Chem.* 14 (2009) 439.
- [5] S.H. van Rijt, P.J. Sadler, *Drug Discov. Today* 14 (2009) 1089.
- [6] C.G. Hartinger, N. Metzler-Nolte, P.J. Dyson, *Organometallics* 31 (2012) 5677.
- [7] F. Wang, J. Xu, K. Wu, S.K. Weidt, C.L. MacKay, P.R.R. Langridge-Smith, P.J. Sadler, *Dalton Trans.* 42 (2013) 3188.
- [8] F. Barragán, P. López-Senín, L. Salassa, S. Betanzos-Lara, A. Habtemariam, V. Moreno, P.J. Sadler, V. Marchán, *J. Am. Chem. Soc.* 133 (2011) 14098.
- [9] F. Wang, A. Habtemariam, E.P.L. Van Der Geer, R. Fernández, M. Melchart, R.J. Deeth, R. Aird, S. Guichard, F.P.A. Fabbiani, P. Lozano-Casal, I.D.H. Oswald, D.I. Jodrell, S. Parsons, P.J. Sadler, *Proc. Natl. Acad. Sci. U.S.A.* 102 (2005) 18269.
- [10] R.E. Morris, R.E. Aird, P. Del Socorro Murdoch, H. Chen, J. Cummings, N.D. Hughes, S. Parsons, A. Parkin, G. Boyd, D.I. Jodrell, P.J. Sadler, *J. Med. Chem.* 44 (2001) 3616.
- [11] M.V. Babak, S.M. Meier, K.V.M. Huber, J. Reynisson, A.A. Legin, M.A. Jakupcic, A. Roller, A. Stukalov, M. Gridling, K.L. Bennett, J. Colinge, W. Berger, P.J. Dyson, G. Superti-Furga, B.K. Keppler, C.G. Hartinger, *Chem. Sci.* 6 (2015) 2449.
- [12] A.A. Nazarov, S.M. Meier, O. Zava, Y.N. Nosova, E.R. Milaeva, C.G. Hartinger, P.J. Dyson, *Dalton Trans.* 44 (2015) 3614.
- [13] A. Weiss, R.H. Berndsen, M. Dubois, C. Müller, R. Schibli, A.W. Griffioen, P.J. Dyson, P. Nowak-Sliwinska, *Chem. Sci.* 5 (2014) 4742.
- [14] C. Scolaro, A. Bergamo, L. Brescacin, R. Delfino, M. Cocchietto, G. Laurency, T.J. Geldbach, G. Sava, P.J. Dyson, *J. Med. Chem.* 48 (2005) 4161.
- [15] H.A. Wee, E. Daldini, C. Scolaro, R. Scopelliti, L. Juillerat-Jeanneret, P.J. Dyson, *Inorg. Chem.* 45 (2006) 9006.
- [16] M. Melchart, A. Habtemariam, S. Parsons, S.A. Moggach, P.J. Sadler, *Inorg. Chim. Acta* 359 (2006) 3020.
- [17] A.F.A. Peacock, M. Melchart, R.J. Deeth, A. Habtemariam, S. Parsons, P.J. Sadler, *Chem. Eur. J.* 13 (2007) 2601.
- [18] C.M. Clavel, E. Păunescu, P. Nowak-Sliwinska, A.W. Griffioen, R. Scopelliti, P.J. Dyson, *J. Med. Chem.* 58 (2015) 3356.
- [19] R. Pettinari, F. Marchetti, F. Condello, C. Pettinari, G. Lupidi, R. Scopelliti, S. Mukhopadhyay, T. Riedel, P.J. Dyson, *Organometallics* 33 (2014) 3709.
- [20] F. Caruso, M. Rossi, A. Benson, C. Opazo, D. Freedman, E. Monti, M.B. Gariboldi, J. Shaulky, F. Marchetti, R. Pettinari, C. Pettinari, *J. Med. Chem.* 55 (2012) 1072.
- [21] R. Fernández, M. Melchart, A. Habtemariam, S. Parsons, P.J. Sadler, *Chem. Eur. J.* 10 (2004) 5173.
- [22] M. Melchart, A. Habtemariam, S. Parsons, P.J. Sadler, *J. Inorg. Biochem.* 101 (2007) 1903.
- [23] A. Habtemariam, M. Melchart, R. Fernández, S. Parsons, I.D.H. Oswald, A. Parkin, F.P.A. Fabbiani, J.E. Davidson, A. Dawson, R.E. Aird, D.I. Jodrell, P.J. Sadler, *J. Med. Chem.* 49 (2006) 6858.
- [24] C.A. Vock, A.K. Renfrew, R. Scopelliti, L. Juillerat-Jeanneret, P.J. Dyson, *Eur. J. Inorg. Chem.* 2008 (2008) 1661.
- [25] A. Romano, C. Conticello, M. Cavalli, C. Vetro, C. Di Raimondo, V. Di Martina, E. Schinocca, A. La Fauci, N.L. Parrinello, A. Chiarenza, F. Di Raimondo, *BioMed Res. Int.* 2014 (2014) 14.
- [26] M.B. Morelli, M. Offidani, F. Alesiani, G. Discepoli, S. Liberati, A. Olivieri, M. Santoni, G. Santoni, P. Leoni, M. Nabissi, *Int. J. Cancer* 134 (2014) 2534.
- [27] P. Govindaswamy, S.M. Mobin, C. Thöne, M.R. Kollipara, *J. Organomet. Chem.* 690 (2005) 1218.
- [28] A. Bruker, Inc. APEX2 (Version 1.08), SAINT (Version 7.03), SADABS (Version 2.11), SHELXTL (Version 6.12), Bruker Advanced X-ray Solutions, Madison, DOI (2004).
- [29] G. Sheldrick, Sadabs, University of Göttingen, Germany Program for Empirical Absorption Correction of Area Detector Data 1996.
- [30] A. Altomare, M.C. Burla, M. Camalli, G.L. Casciaro, C. Giacovazzo, A. Guagliardi, A.G.G. Moliterni, G. Polidori, R. Spagna, *J. Appl. Crystallogr.* 32 (1999) 115.
- [31] G.M. Sheldrick, Program for Crystal Structure Refinement, University of Göttingen, Göttingen, Germany, 2014.
- [32] L.J. Farrugia, *J. Appl. Crystallogr.* 32 (1999) 837.
- [33] A.L. Spek, *J. Appl. Crystallogr.* 36 (2003) 7.
- [34] S. Tabassum, S. Amir, F. Arjmand, C. Pettinari, F. Marchetti, N. Masciocchi, G. Lupidi, R. Pettinari, *Eur. J. Med. Chem.* 60 (2013) 216.
- [35] J.J. Stephanos, *J. Inorg. Biochem.* 62 (1996) 155.
- [36] J.R. Lakowicz, *Principles of Fluorescence Spectroscopy*, Springer Science & Business Media, 2013.
- [37] M. Lee, A.L. Rhodes, M.D. Wyatt, S. Farrow, J.A. Hartley, *Biochemistry* 32 (1993) 4237.
- [38] N. Shahabadi, M. Maghsudi, M. Mahdavi, M. Pourfoulad, *DNA Cell Biol.* 31 (2012) 122.
- [39] L. Quassinti, F. Maggi, L. Barboni, M. Ricciutielli, M. Cortese, F. Papa, C. Garulli, C. Kalogris, S. Vittori, M. Bramucci, *FitoTerapia* 97 (2014) 133.
- [40] A. Tarushi, J. Kljun, I. Turel, A.A. Pantazaki, G. Psomas, D.P. Kessissoglou, *New J. Chem.* 37 (2013) 342.
- [41] Z. Jannesari, H. Hadadzadeh, Z. Amirghofran, J. Simpson, T. Khayamian, B. Maleki, *Spectrochim. Acta Part A: Mol. Biomol. Spectrosc. (Part B)* (2015) 1119.
- [42] F. Marchetti, C. Pettinari, R. Pettinari, *Coord. Chem. Rev.* 249 (2005) 2909.
- [43] F. Marchetti, R. Pettinari, C. Pettinari, *Coord. Chem. Rev.* 303 (2015) 1.
- [44] T. Kruck, *Angew. Chem.* 79 (1967) 27.
- [45] W. Collong, T. Kruck, *Chem. Ber.* 123 (1990) 1655.
- [46] K. Nakamoto, *Infrared and Raman Spectra of Inorganic and Coordination Compounds: Part B: Applications in Coordination, Organometallic, and Bioinorganic Chemistry*, John Wiley & Sons, Inc., 2008.
- [47] R. Wanke, P. Smoleński, M.F.C. Guedes Da Silvan, L.M.D.R.S. Martins, A.J.L. Pombeiro, *Inorg. Chem.* 47 (2008) 10158.
- [48] K.J. Kilpin, C.M. Clavel, F. Edeaf, P.J. Dyson, *Organometallics* 31 (2012) 7031.
- [49] W.J. Geary, *Coord. Chem. Rev.* 7 (1971) 81.
- [50] A. Romerosa, T. Campos-Malpartida, C. Lidrissi, M. Saoud, M. Serrano-Ruiz, M. Peruzzini, J.A. Garrido-Cárdenas, F. García-Maroto, *Inorg. Chem.* 45 (2006) 1289.
- [51] D. Mavrynsky, J. Rahkila, D. Bandarra, S. Martins, M. Meireles, M.J. Calhorda, I.J. Kovács, I. Zupkó, M.M. Hänninen, R. Leino, *Organometallics* 32 (2013) 3012.
- [52] C. Yang, J. Xu, J. Ma, D. Zhu, Y. Zhang, L. Liang, M. Lu, *Photochem. Photobiol. Sci.* 12 (2013) 330.
- [53] H.-Y. Ren, C.-Y. Han, M. Qu, X.-M. Zhang, *RSC Adv.* 4 (2014) 49090.
- [54] A. Gougelet, A. Mansuy, J.-Y. Blay, L. Alberti, C. Vermot-Desroches, *PLoS ONE* 4 (2009) e8026.
- [55] N. Miller, C. RiceEvans, *Redox Rep.* 2 (1996) 161.
- [56] P. Goupy, C. Dufour, M. Loonis, O. Dangles, *J. Agric. Food Chem.* 51 (2003) 615.
- [57] R. Pettinari, F. Marchetti, F. Condello, C. Pettinari, G. Lupidi, R. Scopelliti, S. Mukhopadhyay, T. Riedel, P.J. Dyson, *Organometallics* 33 (2014) 3709.
- [58] E.N. Zaitsev, S.C. Kowalczykowski, *Nucleic Acids Res.* 26 (1998) 650.